

ISSN: 0258-2724

DOI : 10.35741/issn.0258-2724.55.1.33

Research article

Computer and Information Science

**COMPUTATIONAL DESIGN OPTIMIZATION: A COMBINED
DARRIEUS-SAVONIUS WATER TURBINE DESIGN WITH A MODIFIED
BLADE POSITION ON BUCKETS****计算设计优化：桶上的叶片位置经过修改的达里乌斯·萨沃尼乌
斯水轮机组合设计**

Suhartono *, Irjan

Maulana Malik Ibrahim Islamic State University of Malang
Jl Gajayana 50, Malang, Indonesia, suhartono@ti.uin-malang.ac.id**Abstract**

The aim of this study was to determine the optimization of a combined Darrieus-Savonius water turbine design with a modified blade position on buckets. To determine the right position of the blade on the buckets, an analysis of the cut plot pressure on the combined turbine was required. The analysis of the cut plot pressure usually uses the embedded analysis in SolidWorks software to improve the combined water turbine design. This research seeks to propose an additional analysis of the cut plot pressure using an image-processing approach. The image processing approach in the analysis of the cut plot pressure was done by clustering image-based segmentation using the Fuzzy C-Means algorithm. The combined water turbine design used the NACA 0018 blade profile and buckets. Modification of the blades' position on the buckets can improve the turbines' performance. Three variations of the blades' position modifications were employed, and three variations of the turbine design were simulated by SolidWorks software to obtain the cut plot pressure, which, in the form of a digital image on each variation, was analyzed using the Fuzzy C-Means algorithm. Variations of the combined water turbine design were analyzed and tested using SolidWorks and MATLAB software. The results of the study indicate that the variations of the blades' position on the buckets can increase the pressure of the combined water turbine.

Keywords: Blade, Bucket, Savonius, Darrieus, Combined Water Turbine

摘要 这项研究的目的是确定优化的达里厄斯·萨沃纽斯组合式水轮机设计，其叶片在叶片上的位置经过修改。为了确定叶片在叶片上的正确位置，需要对组合式涡轮机上的割线压力进行分析。割地压力的分析通常使用扎实的作品软件中的嵌入式分析来改善组合式水轮机的设计。这项研究试图提出使用图像处理方法来对割地压力进行额外分析。割区压力分析中的图像处理方法是通过使用模糊 C 均值算法对基于图像的分割进行聚类来完成的。组合式水轮机设计使用纳卡 0018 叶片

轮廓和铲斗。修改叶片在叶片上的位置可以提高涡轮机的性能。使用了叶片位置修改的三个变体，并且通过扎实的作品软件对涡轮设计的三个变体进行了模拟，以获得切绘压力，然后以模糊 C-均值算法。使用扎实的作品和 MATLAB 软件对组合式水轮机设计的变化进行了分析和测试。研究表明，叶片在叶片上的位置变化会增加组合式水轮机的压力。

关键词: 叶片，铲斗，萨沃纽斯，达里厄斯，联合水轮机

I. INTRODUCTION

Research on mechanical energy from water flow to produce electrical energy has been carried out by Khan et al. [1]. The development of water turbine geometry consists of two turbines, namely the Darrieus turbine and the Savonius turbine. The blades in the Darrieus turbine utilize the flow of water to obtain lift force. However, the Darrieus turbine has a weakness in that it is difficult to rotate at a low speed. The blade profile for the Darrieus turbine is hydrofoil and based on the National Advisory Committee for Aeronautics (NACA). The NACA modification can provide a large lift force [5]. Blades in the Savonius turbine use water flow to produce compressive power on the blades [2]. The water turbine with the Savonius blade can rotate at speeds of 0.3 m/s [3], and this turbine also has a very high starting torque [4].

There have been some studies on the “combined Darrieus-Savonius water turbine.” The buckets in the Savonius turbine can be integrated with the blades of the Darrieus turbine to improve the weakness of the Darrieus turbine. Sahim, Ihtisan, Santoso and Sipahutar [6] concluded that the power efficiency of the combined Darrieus-Savonius water turbine was better than either the solo Darrieus or Savonius turbines. The combined Darrieus-Savonius water turbine produces an efficiency rate of 66.76% at a water flow rate of 0.637 m/s [7].

Research on “the combined modification of Darrieus-Savonius water turbine” has been conducted by some researchers. Emil Mosonyi stated that the performance of the combined Darrieus-Savonius water turbine could be improved by modifying the combined turbine [8]. In their study, Nakajima and Ikeda [9] concluded that built a water flow simulation in the combined Darrieus-Savonius water turbine using SolidWorks software; the water flow in the simulation used a mass flow rate of 1.499 m³/s as input. The weakness of this research was due to the fact that the parameters of the combined water turbine design were only based on the SolidWorks software. Some aspects, such as how to get other parameters in SolidWorks software,

it is not considered [9]. The parameters involved in the design include the pressure histogram, pressure center, and the clustering of the pressure center. The cut plots that show the pressure were generated by SolidWorks software in the form of digital images. The digital image can see a contour plot of pressure and the pressure is represented by several colors on the plot. To obtain the best turbine design, we analyzed the cut plot pressure to classify the pressure value with the same characteristics in the same domain. In the cut plot that show the pressure, the pressure value was represented in a digital image as colors, and was clustered based on the proximity between the colors [10]. In this research, we clustered the cut plot that show the pressure using the Fuzzy C-Means (FCM) clustering algorithm. The FCM clustering algorithm is a method of clustering which allows one piece of data to belong to two or more clusters, The algorithm can be used to cluster multidimensional data, assigning each point a membership in each cluster center from 0 to 100 percent [11].

After data clustering, we analyzed the cut plot that show the pressure using a histogram to determine the highest pressure from the best turbine design.

II. METHODS

The research employed a computational fluid dynamics (CFD) method using SolidWorks software and the FCM algorithm using MATLAB software. The two methods were used to understand the characteristics of the cut plot pressure on the blades and buckets. The characteristics of the cut plot pressure were pressure clustering, the highest pressure, and the lowest pressure. The characteristics were then presented in graphical forms, diagrams, and contours so that it is easy to determine the best turbine from the various modifications. Figure 1 shows the stages of the research.

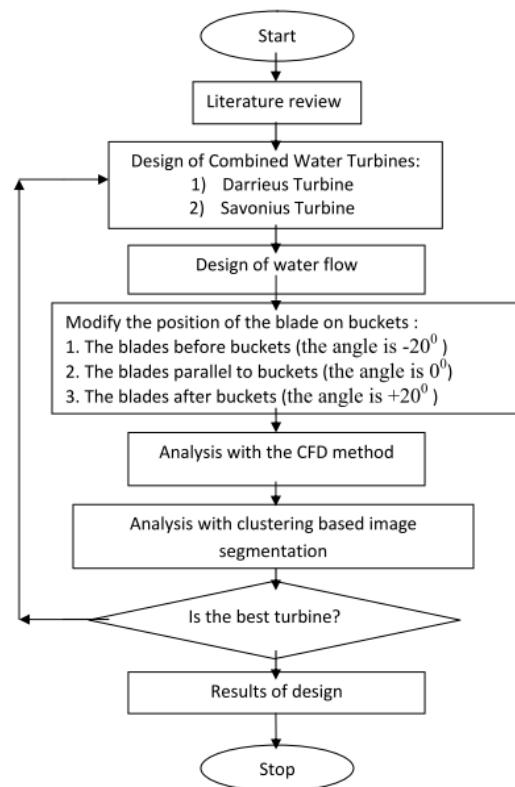


Figure 1. The stages of research

The research process was conducted in two stages as follows: (1) Library research. This stage was aimed at studying the theory of the design and working principles of the Savonius and Darrieus combined water turbines, the theory of fluid mechanics, and rotational motion, and (2) the design of a water turbine which consisted of the combined Darrieus-Savonius water turbine. After the design, a geometric model was made using Solidworks software. (3). The third stage was designing environmental conditions around the turbine using Solidworks software. At this stage, the type of water flow, the value of gravity, domain and room temperature were determined. (4). The fourth stage was turbine modification. At this stage, three angular positions between blade and buckets were made. (5). The fifth stage was the analysis using the CFD method. (6). The sixth stage was the analysis using the FCM method. The result was the degree of the cluster center and some other membership degrees. (7). The seventh stage was the selection process, to determine whether the turbine design is the best. In the next process, which was the eighth stage, if the turbine design was not the best, then a combined water turbine was designed. (8) The eighth stage was the best water turbine design. The parameters in the initial condition were water flow rate of $1.5 \text{ m}^3/\text{s}$ as input models. The water flow rate was based on Reynold's number. The

Reynold's numbers used equation (1) [12] and the Reynold's number was 40000.

$$Re = \frac{\rho v d}{\mu} \quad (1)$$

Water viscosity (μ) was 1.1375×10^{-3} Pa.s, and the water temperature was 28° C . The computational domain was (five times blades length) x (five times blades length) x (five times blades length on the X-axis) for internal flow analysis. The turbine used the NACA 0018 blade profile because the hydrofoil was more stable for small capacities and low water speeds [13]. The blade length was 50% x water turbine diameter; the blade thickness was 20% x blade length, and the number of blades was three, the distance between one blade and another blade is an angle of 120° . The three-dimensional shape of the buckets was half tube and the two-dimensional shape of the buckets was semi-circle to revise the self-starting of the turbine. The semi-circular bucket has been used in research on turbines by Changel et al. [14]. The diameter of buckets was 30% x turbine diameter; the width of buckets was 50% x turbine diameter; and the number of buckets was three; the design of a water turbine with three buckets was used by Sharma [15]. The distance between one bucket and other buckets was an angle of 120° . The buckets were placed between the blades and shaft. The position of the buckets was fused with the shaft.

The study of Kaprawi et al. showed that buckets in combined water turbines provide better performance if the buckets are near the center of the shaft [6]. The positioning of the buckets on blades was investigated by Nakajima et al. [9]. There were three variations of the blade positions on buckets. The first variation was the blades before the buckets (the angle is -20°), the second variation was the blades parallel to buckets (the angle is 0°), and the third variation was the blades after buckets (the angle is $+20^\circ$). The distance between the blades and buckets was 0.1 meter, and the distance of the blades to the bottom wall was 0.1 meter. Darrieus rotor diameter was 1.6 meters; Savonius rotor diameter was 1.6 meters; the width of the Darrieus rotor and the Savonius rotor was 1.6 meters.

Figure 2 shows the design of the Darrieus-Savonius turbine in this research. The combined water turbine design is a water turbine that combines three buckets and three blades. In simulations of the internal water flow flowing blade and buckets, the water flows out through the outlet to environmental conditions. The blade length is 0.4 meter. The blade thickness is 20% x 0.4 meter. The results of Gorlov et all's study indicated that blade thickness affected torque and

turbine rotation; good blade thickness was 20% x blade length. If the blade thickness is large, then the water turbine's rotation is down and the torque is small [16].

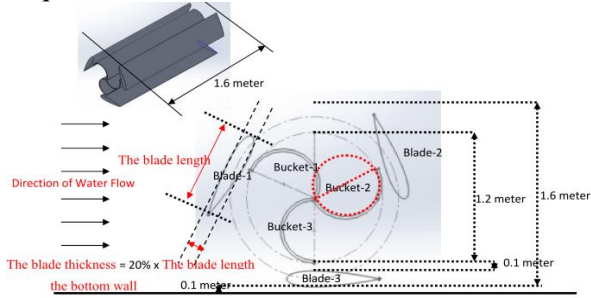


Figure 2. The length and thickness of the blade and buckets

To get a good combined water turbine design, we varied the position of the blade against buckets in this research. The position variations are three, as shown in Figure 3(A), blades are before buckets (the angle is -20°) as design-1, In Figure 3(B), the blades are parallel to buckets (the angle is 0°) as design-2. In Figure 3(C), the blades are after buckets (the angle is $+20^\circ$) as design-3.

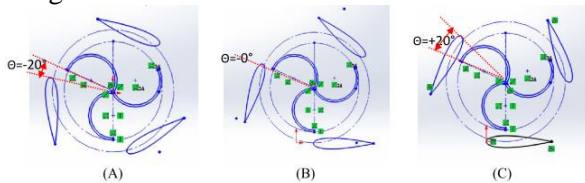


Figure 3. The combined turbine design for blade position on buckets: (A). The angle is -20° as design-1, (B). The angle is 0° as design-2, (C). The angle is $+20^\circ$ as design-3

III. RESULT AND DISCUSSION

In this research, we simulated the cut plot pressure of the water flows dynamically using Solidworks software. The software has the ability to analyze the combined water turbine design related to the water flow. The results of the simulation are data about the water pressure in the turbine, water flow rate, cut plot pressure. We used the data from the simulation to analyze the turbine design on some modifications to get a good turbine. We added several parameters in the analysis process using image processing approach; the parameters were pressure clustering, average pressure value for each clustering. These parameters cannot be generated from the CFD method. The results of the research were a good turbine design; the parameters of the good turbine showed the highest pressure on plot pressure clustering.

A. Analysis of Water Flows Cut Plot Pressure on the Turbine Using Solidworks Software

The initial phase was designing a blade. The number of blades on the turbine was determined

by the value of the Speed Tip Ratio (TSR). To get the TSR value using formula (2) [12], the TSR values for combination turbine were 3 and 4. The number of blades is three, based on Table 1 [12].

$$\lambda = \frac{2\pi r n}{60v} \quad (2)$$

Table 1.
Tip speed ratio guide to the number of blades

Tip speed ratio (λ)	The number of blades (B)
1	6-20
2	4-12
3	3-6
4	2-4
5-8	2-3
8-15	1-2

To get the lift coefficient value using formula (3) [12], the lift coefficient value (Cl) was 1.16032.

$$Cl = \frac{L}{\frac{1}{2}\rho v^2 A} \quad (3)$$

To get the blade length using formula (3) [12], the blade length is 0.3 meter.

$$C = \frac{8\pi r}{B.Cl} (1 - \cos\theta) \quad (4)$$

The external flow conditions are environmental conditions around a combined water turbine. Before the simulation started, we determined the initial condition parameter. The parameter can be shown in Table 2.

Table 2.
The parameter in an initial condition

Thermodynamic parameters	Static pressure	1005 Pa
	Temperature	298.15 K
Velocity parameters	Velocity in X direction	Equation dependency
	Velocity in Y direction	0 m/s
	Velocity in Z direction	0 m/s
	Relative to rotating frame	Off
Turbulence parameter	Intensity	2%
	Length	0.001056

The size of the domain in the direction of the x-axis was 10x the length blade. The domain can get a separation pattern to the turbine more accurate. The Figure 4 shows the domain in turbine design.

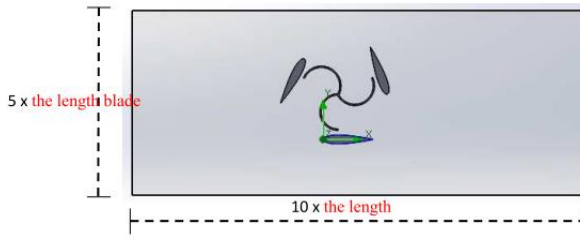


Figure 4. Domain in turbine design

In the domain, the water flow rate was 1.5 m/s in the direction of the positive X axis; the simulation used two dimensional analyses to determine the value of water pressure in the domain area. Turbine modeling used Computer Aided Design (CAD) with Solidworks software. Turbine modeling consisted of blade modeling, buckets modeling, Darrieus turbine diameter, and Savonius turbine diameter. Blade modeling consisted of a blade with NACA type, NACA coordinates, the blade length, the blade thickness, and the number blade. Buckets modeling consisted of the number of buckets, the diameter of the bucket, and the length buckets. The water flow model used the standard epsilon k approach. This model can be used for the hydrodynamic modeling approach and the results are close to the experimental data.

The Solidworks software runs turbine model based on the initial condition. The simulation used an approach to the equation about water flow pressure.

Figure 5 after running animation on Solidworks software for the combined turbine model, the software produced high pressure of flow pressure in center position compared to other positions.

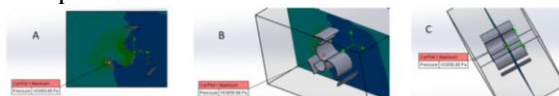


Figure 5. The position of pressure contour in center: A - the front view, B - the side view, C - the top view

The result of the simulation was the cut plot pressure on the turbine in the form of a digital image; the pressure value is represented by the color of the digital image at center position in turbine model. The range for the pressure value is from 101022.98 Pa to 103798.90 Pa. The range for the color value is from blue to red. The range can be seen on the right corner in Figure 6.

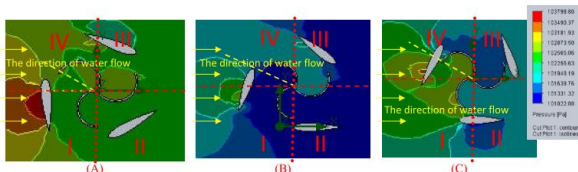


Figure 6. The cut plot pressure at azimuth angle 45° with water flow: (A) the design-1, (B) the design-2, (C) the design-3

Figure 6 shows the cut plot pressure with two-dimensional image. Three turbine designs have different cut plot pressure. The cut plot pressure represents the distribution of the water flow entering through the turbine. Overall, the simulation results have reached convergence, shown by the pressure parameters on the system. As Figures 6A, 6B and 6C indicate, the water flow enters the turbine in quadrants I and IV. The color in quadrants I and IV are brighter, close to red. The red represents high pressure after the water flows out in quadrants II and III. The color is close to blue, which represents low pressure. In Figures 7(A), 7(B) and 7(C), the maximum of cut plot pressure in quadrants I and IV, the minimum of cut plot pressure in quadrants II and III, the water turbine design has the highest pressure in design-2.

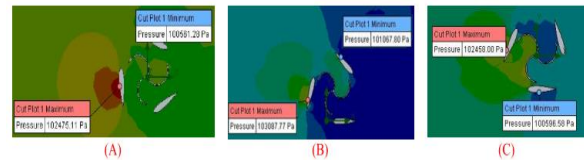


Figure 7. Minimum and maximum of cut plot pressure at azimuth angle 45° with water flow: (A) the design-1, (B) the design-2, (C) the design-3

B. Analysis of Plot Pressure Clustering Using the FCM Algorithm

Pressure cluster analysis is a process for grouping pressure data based on the proximity of the pressure data. In this study, we conducted soft-clustering using the FCM algorithm. FCM algorithm is a clustering method to find cluster centers by minimizing the function of dissimilarity. The digital image of cut plot pressure comes from three designs. The three turbine designs are based on blade positions on buckets. For each turbine design, eight simulations were done. The difference of each simulation is based on the azimuth angle between the water flows to the turbine. Every azimuth angle is $360^{\circ}/8 = 45^{\circ}$. Figure 8 shows the azimuth angle.

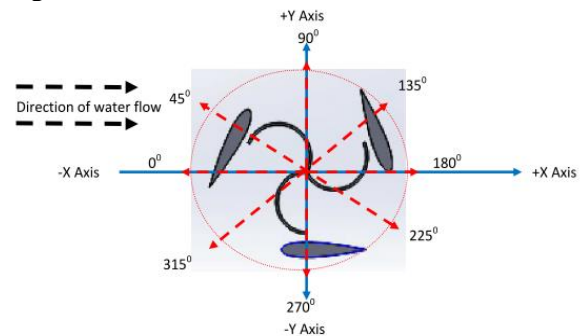


Figure 8. The azimuth angle of the turbine with the direction of water flow

The results of turbine simulation are cut plot pressure as input data in the segmentation process. These results take the form of digital image from Solidworks software. Digital image is a numeric representation from pressure of two-dimensional image. The value of water pressure can be presented in the form of color. The digital image data are RGB image. RGB color space describes colors pattern: red, green, and blue. The colors pattern can be combined in various dimension. RGB image has a size of $n \times m$ (n = image width, m = image height). X_{ij} = data- i (i = 1, 2, ..., n) and data- j (j = 1, 2, ..., m). RGB image is converted to HSV image. HSV describes colors model (hue, saturation, and value). The hue is the color type (red, blue, or yellow), the saturation is the intensity of the color, and the value is the sharpness of the color. HSV digital image is the image color of the wavelength from visible spectrum. The color component in the HSV image can be used as a reference for the introduction of cut plot pressure. The program code conversion from the RGB image to HSV image can be shown in Figure 9.

```
clc; clear; close all;
Img = imread('turbine1.jpg');
figure, imshow(Img), title('Original image');
HSV = rgb2hsv(Img);
figure, imshow(HSV), title('HSV image');
```

Figure 9. Matlab program code for conversion

The RGB image derived from Solidworks software in Figure 10(A); the results of program execution were converted to HSV image in Figure 10(B). The conversion process is in accordance with the direction of the red arrow.

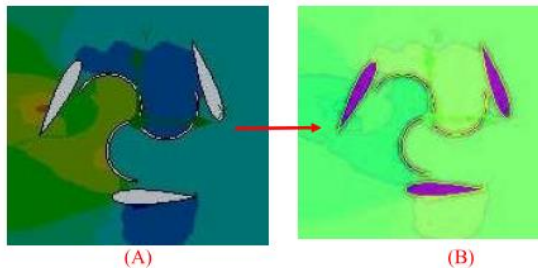


Figure 10. The result of digital image conversion: (A) - Original RGB image, (B) - Conversion HSV image

The number of clusters (c) is three for cut plot pressure. The first cluster is the highest plot pressure, the second cluster is the medium plot pressure, and the third cluster is the low plot pressure. Rank (w) is two, the maximum iteration (Max_{it}) is 100, the smallest error (ξ) is 0.0001, the initial pressure (P_0) is zero, and the initial iteration (t) is one. Random numbers μ_{ik} , i = 1, 2, ..., $n \times m$, k = 1, 2, ..., c were produced. The initial partition matrix element is L and the number of

each column element value in one row is one, the element L uses equation (5).

$$\sum_{i=1}^c L_{ci} = 1 \quad (5)$$

To get the cluster center in the last iteration equation (6) was used.

$$V_{kj} = \frac{\sum_{i=1}^{n \times m} (L_{ik})^2 \cdot X_{ij}}{\sum_{i=1}^{2500} (L_{ik})^2} \quad (6)$$

We iterated until the 12th with an error of 0.00327 to get the last cluster iteration center. Figure 11 shows the iteration program code.

```
figure,
plot(HS(index1,1),HS(index1,2),'ob')
hold on
plot(HS(index2,1),HS(index2,2),'or')
plot(HS(index3,1),HS(index3,2),'oy')
plot(centers(1,1),centers(1,2),'xk','MarkerSize',15,'LineWidth',3)
plot(centers(2,1),centers(2,2),'xk','MarkerSize',15,'LineWidth',3)
plot(centers(3,1),centers(3,2),'xk','MarkerSize',15,'LineWidth',3)
title('Fuzzy c-means clustering')
hold off
```

Figure 11. Matlab program code for plot the cluster center

After the program code in Figure 11 is run with Matlab software, the result is a cluster center of three in Figure 12.

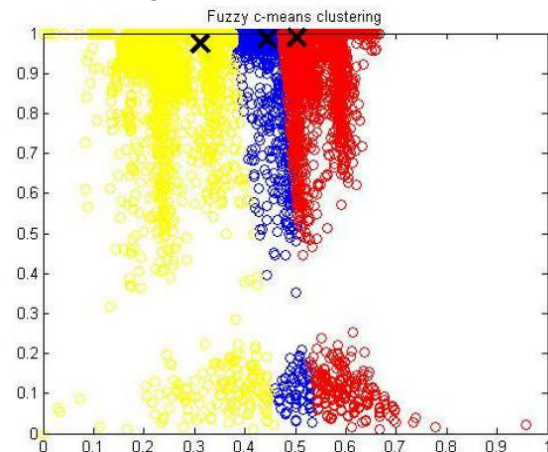


Figure 12. The cluster center plot is three

After the clustering process for the three cluster centers was complete, the process of getting fitness values from the best cluster centers of alliterations was done. Then, the values of each cluster center are mapped in a digital image. The image was labeled according to the clustered index. The program code of the image label can be shown in Figure 13.

```
cluster_idx = zeros(nrows,ncols);
cluster_idx(index1) = 1;
cluster_idx(index2) = 2;
cluster_idx(index3) = 3;
pixel_labels = reshape(cluster_idx,nrows,ncols);
RGB = label2rgb(pixel_labels);
figure, imshow(RGB,[]), title('Image labeled by cluster index');
```

Figure 13. Matlab program code for image label

The Figure 14 shows the results of the cluster image label process.

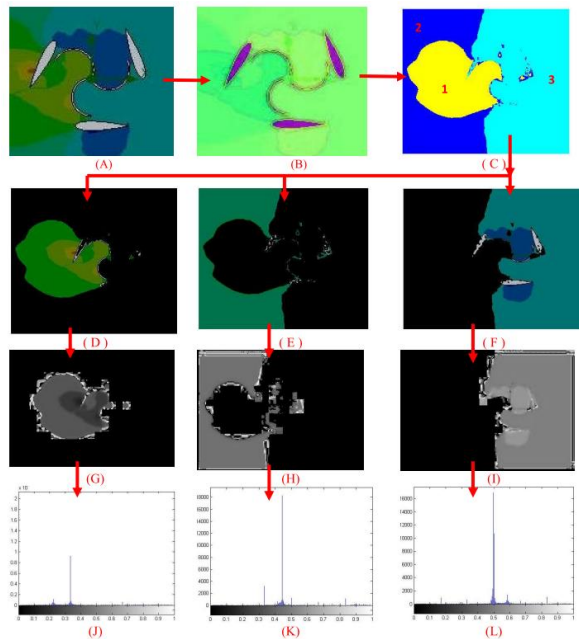


Figure 14. The results of the segmentation of the digital image "contours45.png": (A) - The original RGB image, (B) - The conversion to HSV images, (C) - The ground truth segmentation, (D), (E), (F) - The preprocessed image, (G), (H), (I) - The clustered image in component H, (J), (K), (L) - The histogram image in component H (J) The object-1, (K) - The object-2, (L) - The object-3

Figures 14(A) to 14(L) show images for the stages of the segmentation process using the FCM algorithm. Starting from the original digital image produced by Solidworks software, the process according to the red arrow is the order of segmentation process and the results in every stage. RGB image is a digital image from simulation results using Solidworks software in Figure 14(A). HSV image is a digital image from conversion using Matlab software in Figure 14(B). The ground truth segmentation can know information about clustering in image digital. In Figure 14(C), ground truth data consists of three clusters with three colors; the yellow color (code-1) is cluster-1; cluster-1 is close to the turbine in quadrants I and IV; the blue color (code-2) is cluster-2, and comes before cluster one in quadrants I and IV.

The green color (code-3) is cluster-3. The cluster-3 is after cluster one and cluster two in the quadrants II and quadrants III. The sequence of clusters in the digital images is cluster-1, cluster-2, and cluster-3, according to the direction of the arrow. The next process is a preprocessed image derived by using Statistical Region Merging (SRM) methods, which are techniques for region growing and merging [17]. The result is an object in cluster-1 in Figure 14(D), an object in cluster-2 in Figure 14(E), and an object in cluster-3 in Figure 14(F). Next is a clustering process using the FCM algorithm. The result is x in component

H for object-1 in Figure 14(G); a digital image HSV in component H for object-2 in Figure 14(H); and an HSV image in component H for object-3 in Figure 14(I). The component H can be used to identify pressure because it has the most stable value compared to components S and V, which have spread values.

The next process is analysis using a histogram. The result is a histogram in component H for object-1 in Figure 14(J); for object-2 in Figure 14(K); and for object-3 in Figure 14(L).

Data input in the clustering process is 24 digital images data of cut-plot pressure from the SOLIDWORKS software; the digital images data of cut-plot pressure is based on variations in turbine design. Variations in turbine design can be seen in Figures 3(A), 3(B), and 3(C). Each turbine design has 8 azimuth angle. The 24 digital images data of cut-plot pressure is grouped into three cluster center points: cluster-1 is the center point of high pressure; cluster-2 is the center point of medium pressure; and cluster-3 is the center point of low pressure. The analysis of all three cluster center points can be seen in Figure 15. All three clusters show the pressure value at each turbine position for each turbine design, and we calculated the average of each cluster in each design. Cluster-1 produces the highest average value: the turbine position is 0° , and the turbine is design-2. In design-2 for cluster-2 and cluster-3, both clusters have increased pressure. The combined water turbine design for design-2 is the best turbine design compared to the other positions.

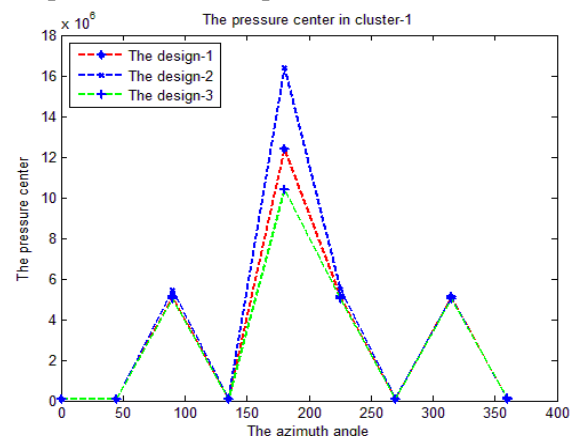


Figure 15. The pressure center in cluster-1

IV. CONCLUSION

In this research, we conducted an analysis using SOLIDWORKS and MATLAB software. Setting the position of the blade against buckets can increase the pressure of the water flow on the combined water turbine. In design-2, all positions of the turbine on the water flow have the highest

average pressure values. In design-2, the position of the blade can help the water flow to the buckets, and the pressure on the buckets is high.

Therefore, it can be concluded that design-1 is the best turbine design compared to the other positions. In design-1, from the combined Darrius-Savonius water turbine, the positions of the blades are parallel to the buckets (the angle is 0^0). For further research, larger-capacity combined water turbines could be modified to get a good combined water turbine design with lower cost.

NOMENCLATURE

v	=	The water flow rate
r	=	The turbine Radius
n	=	The round generator
V_{kj}	=	The cluster center with $k = 1, 2, \dots, c$ and $j = 1, 2, \dots, m \times n$
X_{ij}	=	The data- i ($i = 1, 2, \dots, m$), the data- j ($j = 1, 2, \dots, n$)
μ_{ik}	=	The random numbers with $i = 1, 2, \dots, m \times n$ and $k = 1, 2, \dots, c$
C	=	The blade length
B	=	The number of blade
C_l	=	The lift coefficient
L	=	The lift force
v	=	The water flow rate
A	=	The area
d	=	The turbine diameter
Pa	=	Pascal
Greek Symbols		
μ	=	The water viscosity
ρ	=	The fluid density
θ	=	The angle slant of blade cross section
λ	=	The Tip Speed Ratio

ACKNOWLEDGMENT

The authors would like to thank Institute for Research and Community Service (LP2M) Maulana Malik Ibrahim Islamic State University of Malang for the research grant through the scheme of BOPTN 2019.

REFERENCES

- [1] KHAN, M.J., IQBAL, M.T, and QUAICOE, J.E. (2006) A Technology Review and Simulation Based Performance Analysis of River Current Turbine Systems. In: *Proceedings of the Canadian Conference on Electrical and Computer Engineering, Ottawa, May 2006*. Piscataway, New Jersey: Institute of Electrical and Electronics Engineers, pp. 2288-2293.
- [2] KAMOJI, M.A., KEDARE, S.B., and PRABHU, S. (2009) Experimental investigations on single stage modified Savonius rotor. *Applied Energy*, 86, pp. 1064-1073.
- [3] SARMA, N.K., BISWAS, A., and MISRA, R.D. (2014) Experimental and computational evaluation of Savonius hydrokinetic turbine for low velocity condition with comparison to Savonius wind turbine at the same input power. *Energy Conversion and Management*, 83, pp. 88-98.
- [4] KEDARE, S.B. and PRABHU, S. (2008) Experimental Investigations on the Effect of Overlap Ratio and Blade Edge Conditions on the Performance of Conventional Savonius Rotor. *Wind Engineering*, 32 (2), pp. 163-178.
- [5] HAU, E. (2003) Wind-turbines fundamentals, technologies, application, economics [book review]. *IEEE Electrical Insulation Magazine*, 19 (2), pp. 48-48.
- [6] SAHIM, K., IHTISAN, K., SANTOSO, D., and SIPAHUTAR, R. (2014) Experimental Study of Darrius-Savonius Water Turbine with Deflector: Effect of Deflector on the Performance. *International Journal of Rotating Machinery*, 2014, pp. 1-6.
- [7] MAHMUD, S., SAMPEBATU, L., and CIAYADI KWANG, S. (2017) Mechanical power efficiency of modified turbine blades. *AIP Conference Proceedings*, 1801 (1), pp. 1-8.
- [8] MOSONYI, E. (1987) *Water Power Development: Vol. 1. Low-Head Power Plants*. Budapest: Akadémiai Kiadó.
- [9] NAKAJIMA, M., IIO, S., and IKEDA, T. (2008) Performance of Double-Step Savonius Rotor for Environmentally Friendly Hydraulic Turbine. *Journal of Fluid Science and Technology*, 3 (3), pp. 410-419.
- [10] PAL, N. (2017) A Primer on Cluster Analysis: 4 Basic Methods That (Usually) Work [Book Review]. *IEEE Computational Intelligence Magazine*, 12 (4), pp. 98-100.
- [11] GHARIEB, R.R., GENDY, G., and ABDELFATTAH, A. (2016) Image Segmentation Using Fuzzy C-Means Algorithm Incorporating Weighted Local Complement Membership and Local Data Distances. In: *Proceedings of the 2016 World Symposium on Computer Applications &*

Research, Cairo, March 2016. Piscataway, New Jersey: Institute of Electrical and Electronics Engineers, pp. 6-11.

[12] ANDERSON, J.D. (2011) *Fundamentals of Aerodynamics*. New York: McGraw-Hill.

[13] CIANETTI, F., CASTELLANI, F., ASTOLFI, D., BECCHETTI, M., BERNO, F., and CETRINI, A. (2018) Experimental and Numerical Vibrational Analysis of a Horizontal-Axis Micro-Wind Turbine. *Energies*, 11 (2), pp. 3-16.

[14] CENGEL, Y., TURNER, R., and SMITH, R. (2001) *Fundamentals of Thermal-Fluid Sciences*. New York: McGraw-Hill.

[15] GUPTA, R. and SHARMA, K.K. (2011) Flow Physics of a Three-Bucket Savonius Rotor Using Computational Fluid Dynamics (CFD). *International Journal of Research in Mechanical Engineering and Technology*, 1 (1), pp. 46-51.

[16] GORLOV, A. (1998) *Development of the helical reaction hydraulic turbine*. [Online] United States Department of Energy, Office of Scientific and Technical Information. Available from: <https://www.osti.gov/biblio/666280-D6NWM1/webviewable/> [Accessed 15/02/20].

[17] NOCK, R., and NIELSEN, F. (2004) Statistical Region Merging. *IEEE Transactions on Pattern Analysis and Machine Intelligence*, 26 (11), pp. 1452-1458.

参考文献:

[1] KHAN, M.J., IQBAL, M.T. 和 QUAICOE, J.E. (2006) 基于技术回顾和基于仿真的河流水轮机系统性能分析。于：2006年5月在渥太华举行的加拿大电气与计算机工程会议论文集。新泽西州皮斯卡塔维：电气与电子工程师协会，第2288-2293页。

[2] KAMOJI, M.A., KEDARE, S.B. 和 PRABHU, S. (2009) 对单级改良萨沃纽斯转子的实验研究。应用能源，86，第1064-1073页。

[3] N.K. SARMA, A. BISWAS 和 R.D. MISRA (2014) 在相同输入功率下与萨沃纽斯风力涡轮机相比，萨沃纽斯流体动力涡轮机在低速条件下的实验和计算评估。能源转换和管理，83，第88-98页。

[4] KEDARE, S.B. 和 PRABHU, S. (2008) 对重叠比和叶片边缘条件对传统萨沃纽斯转子性能的影响的实验研究。风力工程，32 (2)，第163-178页。

[5] HAU, E. (2003) 风力发电机的基本原理，技术，应用，经济学 [书评]。电气工程师学会电气绝缘杂志，19 (2)，第48-48页。

[6] SAHIM, K., IHTISAN, K., SANTOSO, D. 和 SIPAHUTAR, R. (2014) 带有偏转器的达里厄斯·萨沃纽斯水轮机的实验研究：偏转器对性能的影响。国际旋转机械杂志，2014年，第1-6页。

[7] MAHMUD, S., SAMPEBATU, L. 和 CIAYADI KWANG, S. (2017) 改进型涡轮机叶片的机械功率效率。AIP会议论文集，1801 (1)，第1-8页。

[8] MOSONYI, E. (1987) 水力发展：第一卷。1.低水头发电厂。布达佩斯：学术出版商。

[9] 中岛美纪, IIO 和 S. IKEDA (2008) 环保型水轮机用双步式萨沃纽斯转子的性能。流体科学与技术杂志，3 (3)，第410-419页。

[10] PAL, N. (2017) 聚类分析入门：(通常)有效的4种基本方法[书评]。电气工程师学会计算智能杂志，12 (4)，第98-100页。

[11] GHARIEB, R.R., GENDY, G. 和 ABDELFAH, A. (2016) 使用结合加权局部互补成员和局部数据距离的模糊C均值算法进行图像分割。于：2016年世界计算机应用与研究世界研讨会论文集，开罗，2016年3月。新泽西州皮斯卡塔维：电气与电子工程师协会，第6-11页。

[12] ANDERSON, J.D. (2011) 空气动力学基础。纽约：麦格劳-希尔。

[13] CIANETTI, F., CASTELLANI, F., ASTOLFI, D., BECCHETTI, M.,

BERNO, F. 和 CETRINI, A. (2018) 水平轴微风轮机的实验和数值振动分析。能源, 11 (2), 第 3-16 页。

[14] CENGEL, Y., TURNER, R. 和 SMITH, R. (2001) 热流体科学基础。纽约: 麦格劳-希尔。

[15] R. GUPTA 和 K.K. SHARMA。 (2011) 使用计算流体力学 (差价合约) 的三桶式萨沃纽斯转子的流物理学。国际机械工程与技术研究杂志, 1 (1), 第 46-51 页。

[16] GORLOV, A. (1998) 螺旋反应水轮机的开发。 [在线]美国能源部科学技术信息办公室。可从以下网站获得: <https://www.osti.gov/biblio/666280-D6NWM1/webviewable/> [访问时间: 20/02/15]。

[17] NOCK, R. 和 NIELSEN, F. (2004) 统计区域合并。电气工程师学会模式分析与机器智能交易, 26 (11), 第 1452-1458 页。